 CMES, vol.4, no.1, pp.197-212, 2003

A Boundary Element Method for Acoustic Scattering from Non-axisymmetric and Axisymmetric Elastic Shells

J. P. Agnantiaris[1] **and D. Polyzos**[1,2]

Abstract: A Boundary Element Method (BEM), for the three-dimensional solution of both non-axisymmetric and axisymmetric coupled acoustic-elastic problems in the frequency domain, is presented. The present BEM makes use of the Burton and Miller integral equation for infinite acoustic spaces, while elastic structures are dealt with the standard boundary integral equation of elastodynamics. The axisymmetric formulation involves the use of the fast Fourier transform algorithm. Highly accurate numerical algorithms are used for the evaluation of singular integrals, while nearly singular integrals are treated, also with high accuracy, through the use of practical numerical techniques, for both the axisymmetric and non-axisymmetric cases. Two representative numerical examples are solved, that demonstrate the accuracy of the present BEM, while interesting observations are reported about its convergence properties, when arbitrarily shaped shell scatterers are under consideration.

keyword: 3-D acoustic scattering, Fluid-shell structure interaction, boundary elements, axisymmetry.

1 Introduction

The scattering of sound waves by elastic shell structures immersed in liquid is a problem of great significance for many engineering applications belonging in the area of underwater acoustics. Several analytical, semi-analytical and numerical methodologies are available in the literature for the treatment of such a scattering problem. Analytical or semi-analytical methods have the disadvantage of solving an underwater acoustics scattering problem only under various limitations in shape, size and composition of the target. On the other hand, numerical methods, such as the finite element method (FEM), the boundary element method (BEM), and the hybrid finite-boundary element method (FEM/BEM) can solve with no significant restrictions very complicated scattering problems. However, it should be mentioned that despite their limitations, analytical methods appear to have the advantage of providing solutions or approximations quickly and with low computational cost, over computational ones, for many practical applications [Gaunaurd and Werby (1990)]. Also, for simple shapes, analytical methods provide valuable accurate solutions, with the aid of which the accuracy and the efficiency of numerical methods are assessed. Similarly, the semi-analytical method of T-matrix approach [Waterman (1969); Tobocman (1985)] has, to date, solved difficult multi-scattering problems for which solutions by a computational method would be prohibitive.

The BEM is a well-known and powerful numerical tool for solving frequency domain acoustic radiation and scattering problems [Rego Silva (1994); Ciskowski and Brebbia (eds) (1991)]. Because of utilizing the standard Helmholtz integral equation, the BEM is ideally suited to treat such exterior problems, since it takes automatically into account the far-field radiation conditions reducing thus the dimensionality of the problem by one [Seybert, Wu, Wu (1988)]. This means that three-dimensional (3-D) scattering problems are accurately solved by discretizing only the two-dimensional (2-D) surface of the scatterer and not the interior plus the infinitely extended exterior acoustic domain as the FEM does. In the case, where the problem is characterized by an axisymmetric geometry, the BEM reduces further the dimensionality of the problem, requiring just a discretization along the meridional line of the body. On the other hand, the FEM is ideal for handling problems dealing with the dynamic behavior of very complicated elastic shell structures. Thus, in the literature, the most popular method for treating coupled acoustic-structural radiation and scattering problems is that of the hybrid FEM/BEM (FEM for the structure, BEM for the acoustic domain), where the

[1] Department of Mechanical and Aeronautical Engineering
Applied Mechanics Laboratory
University of Patras, GR-26500 Patras, Greece
[2] nstitute of Chemical Engineering and High Temperature Chemical Processes-FORTH, GR-26500,Patras, Greece

advantages of the two methods are appropriately combined. Here one can mention the representative works of Schenk and Benthien (1989), Everstine and Henderson (1990), Zeng and Zhao (1994) and Veksler, Lavie, Dubus (2000), Lie, Yu, Zhao (2001), Gaul, Fischer and Nackenhorst (2002). However, in the recent publications of Burnett and Holford (1998) and Chen and Liu (1999) some drawbacks of the two methods have been successfully circumvented and only the FEM in the first and the BEM in the later work have been efficiently used for the solution of fluid-shell structure interaction scattering problems. This fact indicates that as computers become faster and numerical algorithms more optimized, individual numerical methods overcome their drawbacks and are continually improved in efficiency.

In the context of the BEM, the main difficulty in the application of the method to acoustic radiation and scattering problems is the well-known "ficticious eigenfrequency difficulty" where the exterior boundary integral solution becomes non-unique at some eigenfrequencies associated with interior boundary value problems. Several methodologies for eliminating this problem have been proposed, to date, in the literature. Among them, the most widely used are those of the coupled Helmohltz integral equation formulation (CHIEF), proposed by Schenck (1968), and the combined integral equation method proposed by Burton and Miller (1971), known in the literature as the Burton and Miller formulation (BMF).

The CHIEF utilizes the standard Helmholtz integral equation (SHIE) and circumvents the eigenfrequency difficulty by considering additional collocation points in the interior domain. The main problem with this methodology is the selection of the interior points. More precisely, it has been proven [Seybert and Rengarajan (1987)] that the CHIEF provides eigenfrequency free SHIE only when at least one of the interior collocation points does not lie on a nodal surface (eigenmode corresponding to an eigenfrequency of the related interior problem). This requirement, in conjunction with the fact that the nodal surfaces are not known "*a priori*", increases the computational cost of the CHIEF, since several internal points should be considered, in order to have the high probability of taking at least one point beyond the nodal surfaces.

Burton and Miller have proven that the linear combination of the SHIE and its normal derivative (DHIE) provides unique solutions, for all frequencies and regardless of the type of boundary conditions, if the coupling complex coefficient has non-zero imaginary part. On the other hand, Krishnasamy, Rizzo and Liu (1994) have shown that for exterior acoustic problems, the degeneracy, which happens when the SHIE or the DHIE are applied to the two surfaces of a very thin scatterer, can be removed by employing the BMF. These two important characteristics of the combined Helmholtz integral equation make the BMF to be mathematically the most desirable approach for treating acoustic scattering and radiation problems. From a computational point of view however, the BMF has the disadvantage of requiring the treatment of hyper-singular integrals coming from the DHIE. Although several analytical semi-analytical and numerical techniques dealing with the accurate evaluation of hyper-singular integrals are available in the literature [Tanaka, Sladek, Sladek (1994)], the numerical complexity on treating this kind of integrals remains, since the DHIE exists only at surface field points where the density functions of the corresponding hyper-singular integrals are Holder continuously differentiable ($C^{(1)}$-continuity difficulty) [Colton, Kress (1983)]. For a BEM code, this means that in the discretization process, only boundary elements, which guarantee the just mentioned continuity requirement, should be chosen. One such choice is the use of Overhauser elements [Tanaka, Sladek, Sladek (1994); Sladek, Sladek (1999)], but these elements need more than one degree of freedom per node, leading thus to large systems of equations to be solved. Of course there is always the alternative of using constant elements, which also fulfil the $C^{(1)}$-continuity requirement, but at the cost of lower spatial and field interpolation.

To avoid the C^1 continuity difficulty, Cunefare, Koopman and Brod (1989) and Miller, Thomas, Moyer, Huang and Uberall (1991) proposed the use of the so-called "off-boundary approach" where the collocation points are placed on an internal surface usually being geometrically similar to the real boundary of the scattering or radiation problem. Although this methodology avoids the treatment of any kind of singular integrals, appears the disadvantage of requiring a parametric study for the optimum selection of the internal collocation points. Rego Silva (1994) circumvents the problem by using full-discontinuous, eight-node, quadratic elements in which the collocation points are placed inside the element, where the density function of the hyper-singular integral is infinitely smooth. However, the use of fully-

discontinuous elements increases drastically the computational cost of the boundary element solution. A good alternative idea to that of using discontinuous elements is the modified Burton and Miller algorithm (MBMA) proposed by Ingber and Hickox (1992). According to this methodology 9-noded quadratic continuous elements are used, and the final BEM algebraic system of equations is obtained by collocating the SHIE at the inter-element nodes and the integral equation, imposed by the BMF, at the interior ninth node. Another technique is that proposed by Wilde, Aliabadi and Power (1996), where the C^1-continuity difficulty is circumvented by employing a new interpolation scheme based on the nodal values of all elements containing the collocation point. The main problem with this methodology is the introduction of restrictions on the BEM mesh as well as on the location of the collocation points where the BMF is applied. Finally, several researchers avoid the problem by employing regularization techniques [Chien, Rajiah, Atluri (1990); Chen, Liu (1999); Liu (2000)] on both SHIE and DHIE, before discretization, relaxing thus the smoothness requirements for DHIE.

In the BEM treatment of an acoustic wave scattering problem by an elastic shell structure, the dynamic behaviour of the elastic medium is simulated through the standard elastodynamic integral equation [Manolis, Beskos (1988)] (SEIE). In that case another difficulty to be dealt with is appeared. This difficulty concerns the numerical evaluation of the nearly singular integrals appearing in the SEIE when thin elastic structures are considered and a field point is very closed to the surface on which the integration is performed. Many methods have also been proposed for the accurate and efficient evaluation of those integrals. The most known are those which utilize techniques like transformation to line integrals after regularization [Liu (1998); Mukherjee, Chati, Shi (2000)], element subdivision [Lachat, Watson (1976)], co-ordinate mappings [Telles (1987); Huang, Cruse (1993), Yang (2000); Sladek, Sladek, Tanaka (2000)] and Taylor expansions around the singularity [Huber, Rieger, Haas, Rucker (1997), Ma and Kamiya (2002)].

The present work addresses a direct frequency domain BEM for solving 3-D axisymmetric and non-axisymmetric, coupled acoustic-structural scattering problems, where the scatterers are shell-like structures. The SEIE is used for the elastic structure, while the BMF is employed for the exterior acoustic domain, in order the ficticious eigenfrequency difficulty to be avoided. For the case of non-axisymmetric scatterers the C^1-continuity difficulty is circumvented by means of the MBMA. Thus, 9-noded isoparametric, conforming elements are used for the discretization of the acoustic-elastic interface and 8-noded elements for the rest of the boundary surface of the shell structure. For axisymmetric geometries an accurate and efficient boundary element/Fast Fourier transform (FFT) methodology, which combines effectively the works of Tsinopoulos, Kattis, Polyzos and Beskos (1999) and Tsinopoulos, Agnantiaris, Polyzos (1999), is proposed. According to this methodology, the boundary quantities of the problem are expanded in complex Fourier series, with respect to the circumferencial direction. Due to this expansion, each boundary integral involved in the SEIE and the BMF is reduced to a line integral along the surface generator of the body and an integral over the angle of revolution. The first integral is evaluated through Gauss quadrature, by employing a 2-D boundary element methodology. The integration over the circumferential direction is performed simultaneously for all the Fourier coefficients through the FFT. The proposed here axisymmetric technique does not suffer from the C^1-continuity difficulty and thus the surface generator of the scatterer can be discretized into 3-noded conforming quadratic line elements.

Highly accurate numerical algorithms, proposed by Guiggiani and co-workers [Guiggiani (1992), Guiggiani, Krishnasamy, Rudolphi and Rizzo (1992)] for the direct evaluation of the strongly singular and hypersingular integrals are employed here for both the axisymmetric and non-axisymmetric cases. Nearly singular integrals are evaluated numerically, with increased accuracy (0.01%), through a practical integration technique, depending on the parameter D_{ek}/l_e with D_{ek} being the minimum distance between the field point and the boundary element in which the integration is performed, and l_e the biggest element side. More precisely, for $D_{ek}/l_e < 0.2$ the integrals are expressed in a local polar co-ordinate system (R,θ) and the integration is performed through Gauss quadrature with 4 and K integration points in angular and radial direction, respectively. For $D_{ek}/l_e > 2$ the integrals are evaluated with the aid of standard Gauss quadrature utilizing $\Lambda \times \Lambda$ integration points. Both K and Λ are functions of D_{ek}/l_e and are automatically determined via simple relations proposed here.

Finally, two representative numerical examples concerning the scattering of a plane wave by a spherical and a cylindrical with hemispherical end-cups shell are presented. The aim of these two numerical examples is twofold: first to demonstrate the high accuracy of the proposed here direct frequency domain BEM and second to illustrate some very interesting remarks concerning the convergence of the BEM at resonances occurring in the intermediate frequency range.

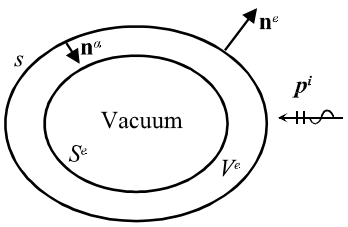

Figure 1 : Elastic shell illuminated by a plane acoustic wave

2 Formulation of the problem

2.1 Boundary integral equations

When dealing with sound-shell structure interaction problems, a hybrid state is considered, which involves coupling between the motion of an elastic shell and the corresponding domain where acoustic waves are propagating. More specifically, when a linearly elastic, isotropic and homogeneous body of volume V^e is submerged into an infinite acoustic domain (see Fig.1), then, by assuming harmonic time dependence of the displacement and pressure fields, the governing equation describing the motion of the elastic body, is the well known Navier-Cauchy equation [Manolis and Beskos (1988)], while the one valid for the wave propagation in the acoustic domain is the Helmholtz equation [Rego Silva (1994)].

The complete boundary value problem, demands the implication of appropriate boundary conditions defined over the elastic boundary S^e and the interface s between the two media i.e.

$$\left.\begin{array}{ll} \mathbf{t}(\mathbf{x}) = \mathbf{0} & \\ \mathbf{u}(\mathbf{x}) \cdot \mathbf{n}^e(\mathbf{x}) = -\frac{1}{\rho_0 \omega^2} \cdot \frac{\partial p(\mathbf{x})}{\partial \mathbf{n}^\alpha(\mathbf{x})} & \\ \mathbf{t}(\mathbf{x}) \cdot \mathbf{n}^\alpha(\mathbf{x}) = p(\mathbf{x}) & \end{array}\right\} \begin{array}{l} \mathbf{x} \in S^e \\ \\ \mathbf{x} \in s \end{array} \tag{1}$$

where $\mathbf{n}^e$, $\mathbf{n}^\alpha$ are the unit normal vectors at the surface point $\mathbf{x}$, defined by the elastic and acoustic domain, respectively, ρ_0 is the density of the acoustic medium and ω is the angular frequency of oscillation. The vectors $\mathbf{u}$ and $\mathbf{t}$ stand for the displacement and traction vectors on the elastic side, while the scalar functions $p$and $\partial p/\partial \mathbf{n}^a$ refer to the acoustic pressure and its normal gradient on the acoustic side, respectively.

The starting point for the solution of any structural-acoustic problem via the BEM, is to reformulate it in terms of the appropriate system of integral equations. To this end, the integral equation valid for the elastic domain is the SEIE

$$c_1(\mathbf{x}) \cdot \mathbf{u}(\mathbf{x}) = \int_{S^e+s} [\mathbf{u}^*(\mathbf{x},\mathbf{y}) \cdot \mathbf{t}(\mathbf{y}) - \mathbf{t}^*(\mathbf{x},\mathbf{y}) \cdot \mathbf{u}(\mathbf{y})] \, dS(\mathbf{y}), \tag{2}$$

where $\mathbf{x}$ represents the field point at which the displacement field $\mathbf{u}$ is evaluated and $\mathbf{y}$ the boundary source points at which the density functions are defined. The tensors $\mathbf{u}^*(\mathbf{x},\mathbf{y})$ and $\mathbf{t}^*(\mathbf{x},\mathbf{y})$ are the fundamental displacement and traction of the Navier-Cauchy elastodynamic equation [Manolis and Beskos (1988)]. The corresponding integral equation valid for the acoustic domain is the SHIE, which is written as

$$c_2(\mathbf{x}) \cdot p(\mathbf{x}) = \int_s \left[G(\mathbf{x},\mathbf{y}) \frac{\partial p(\mathbf{y})}{\partial \mathbf{n}_\mathbf{y}} - \frac{\partial G(\mathbf{x},\mathbf{y})}{\partial \mathbf{n}_\mathbf{y}} p(\mathbf{y}) \right] dS(\mathbf{y}) + p^i(\mathbf{x}), \tag{3}$$

with G(**x**,**y**) being the fundamental solution of the Helmholtz equation [Rego Silva (1994)], $\frac{\partial G(\mathbf{x},\mathbf{y})}{\partial \mathbf{n}_y}$ is its normal derivative, with respect to point **y**, and $p^i(\mathbf{x})$ is the incident pressure. The scalars $c_1(\mathbf{x})$ and $c_2(\mathbf{x})$ appearing in (2) and (3) are the well known jump coefficients, which obtain the values $c_1(\mathbf{x})$=1, $c_2(\mathbf{x})$=0 for $\mathbf{x} \in V^e$, $c_1(\mathbf{x})$=0, $c_2(\mathbf{x})$=1 for exterior to the scatterer points and $c_1(\mathbf{x})$=1/2 for $\mathbf{x} \in S^e \cup s$, $c_2(\mathbf{x})$=1/2 for $\mathbf{x} \in s$, for a smooth boundary.

It is well known from the literature, that equation (3), when it is applied for the modelling of exterior problems fails to provide a unique solution at certain frequencies,

which are called fictitious eigenfrequencies. To circumvent this difficulty, the present work employs the BMF [Burton and Miller (1971)], which is a linear combination of equation (3) and its normal derivative, with respect to the field point **x**. This equation is written as

$$
\begin{aligned}
& c\,(\mathbf{x})\left[p\,(\mathbf{x})+\varepsilon\frac{\partial p\,(\mathbf{x})}{\partial \mathbf{n}_{\mathbf{x}}}\right] \\
& \int_s\left[\left\{G(\mathbf{x},\mathbf{y})+\varepsilon\frac{\partial G(\mathbf{x},\mathbf{y})}{\partial \mathbf{n}_{\mathbf{x}}}\right\}\frac{\partial p\,(\mathbf{y})}{\partial \mathbf{n}_{\mathbf{y}}}\right. \\
& \left.-\left\{\frac{\partial G(\mathbf{x},\mathbf{y})}{\partial \mathbf{n}_{\mathbf{y}}}+\varepsilon\frac{\partial^2 G(\mathbf{x},\mathbf{y})}{\partial \mathbf{n}_{\mathbf{x}}\partial \mathbf{n}_y}\right\}\right] p\,(\mathbf{y})\,dS\,(\mathbf{y}) \\
& +\left[p^i\,(\mathbf{x})+\varepsilon\frac{\partial p^i(\mathbf{x})}{\partial \mathbf{n}_{\mathbf{x}}}\right] \qquad (4)
\end{aligned}
$$

where the coupling coefficient ε takes the value i/k, where $i=\sqrt{-1}$ and k is the acoustic wavenumber.

2.1.1 *Boundary integral equations for axisymmertric scatterers*

In case when the coulped acoustic-structural scattering problem is characterised by an axisymmetric geometry with respect to the X_3 axis, of a rectangular coordinate system (X_1,X_2,X_3), then the integral equations (2) and (4) can be reduced to integral equations defined only on the boundary surface generator line $\Gamma=\Gamma_e+\gamma$ of the structure and over the angle of revolution φ (see Fig.2) of the associated cylindrical coordinate system (ρ,φ, z).

Here, the line Γ_e stands for the generator of the elastic boundary S^e and line γ for the elastic/acoustic interface generator. All the displacement and traction vectors as well as the fundamental solution tensors in Eq.(2) are expressed in the cylindrical orthogonal basis, through the operation of an orthogonal transformation matrix relating the cylindrical and rectangular components of a vector. Of course this is not the case for the scalar quantities in Eq.(4), where the axisymmetric nature of the free space Green's function G permits a straightforward expression of those equations, in terms of the cylindrical co-ordinates. Next, all the boundary quantities of the two integral equations, the boundary conditions and the incident acoustic wave, are expanded into discrete complex Fourier series with respect to the polar angle φ. The series summation is performed over a number of harmonics, which are enough to express the, in general non-axisymmetric, incident field over the circumference with a reasonable accuracy. All the expansion coefficients are computed through the FFT algorithm [Cooley, Tukey (1965)]. Inserting all the Fourier expansions into Eqs(2) and (4) and invoking orthogonality arguments, one obtains the final axisymmetric integral equations for the n^{th} Fourier boundary coefficient as:

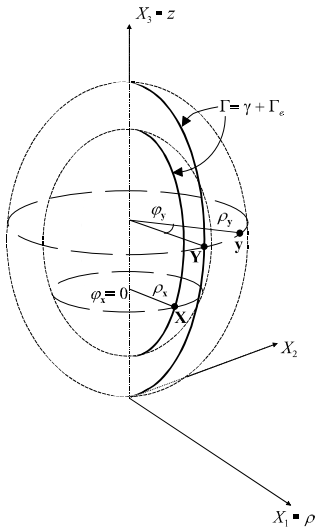

Figure 2 : Axisymmetric shell and its geometry

$$
\begin{aligned}
& c\,(\mathbf{X})\cdot\mathbf{u}_n^c\,(\mathbf{X})=\int_{\Gamma_e+\gamma}\rho_{\mathbf{Y}}\mathbf{U}^{(n)}\,(\mathbf{X},\mathbf{Y})\cdot\mathbf{t}_n^c\,(\mathbf{Y})\,d\Gamma_{\mathbf{Y}} \\
& -\int_{\Gamma_e+\gamma}\rho_{\mathbf{Y}}\mathbf{T}^{(n)}\,(\mathbf{X},\mathbf{Y})\cdot\mathbf{u}_n^c\,(\mathbf{Y})\,d\Gamma_{\mathbf{Y}} \qquad (5) \\
& c\,(\mathbf{X})\left[p_n\,(\mathbf{X})+\varepsilon\frac{\partial p_n(\mathbf{X})}{\partial \mathbf{n}_{\mathbf{X}}}\right]= \\
& \int_{\Gamma_e+\gamma}\rho_{\mathbf{Y}}\left\{G^{(n)}\,(\mathbf{X},\mathbf{Y})+\varepsilon\frac{\partial G^{(n)}\,(\mathbf{X},\mathbf{Y})}{\partial \mathbf{n}_{\mathbf{X}}}\right\}\frac{\partial p_n(\mathbf{Y})}{\partial \mathbf{n}_{\mathbf{Y}}}d\Gamma_{\mathbf{Y}} \\
& -\int_{\Gamma_e+\gamma}\rho_{\mathbf{Y}}\left\{\frac{\partial G^{(n)}\,(\mathbf{X},\mathbf{Y})}{\partial \mathbf{n}_{\mathbf{Y}}}+\frac{\partial^2 G^{(n)}\,(\mathbf{X},\mathbf{Y})}{\partial \mathbf{n}_{\mathbf{X}}\partial \mathbf{n}_{\mathbf{Y}}}\right\}p_n(\mathbf{Y})d\Gamma_{\mathbf{Y}} \\
& +\left[p_n^i\,(\mathbf{X})+\varepsilon\frac{\partial p_n^i(\mathbf{X})}{\partial \mathbf{n}_{\mathbf{X}}}\right] \qquad (6)
\end{aligned}
$$

where ρ_Y is the radial co-ordinate of the field point. All the kernels $\mathbf{U}^{(n)}(\mathbf{X},\mathbf{Y})$,$\mathbf{T}^{(n)}(\mathbf{X},\mathbf{Y})$, $\left\{G^{(n)}(\mathbf{X},\mathbf{Y})+\varepsilon\frac{\partial G^{(n)}(\mathbf{X},\mathbf{Y})}{\partial \mathbf{n_X}}\right\}$ and $\left\{\frac{\partial G^{(n)}(\mathbf{X},\mathbf{Y})}{\partial \mathbf{n_Y}}+\varepsilon\frac{\partial G^{(n)}(\mathbf{X},\mathbf{Y})}{\partial \mathbf{n_Y}}\right\}$ in the above equations are written in general form, as integrals of the transformed fundamental solutions over the circumferential direction ϕ like

$$F^{(n)}(\mathbf{X},\mathbf{Y})=\int_0^{2\pi} F_c^*(\mathbf{X},\mathbf{Y},\varphi)e^{in\varphi}d\varphi \tag{7}$$

with $\mathbf{X}(\rho_x,\ z_x)$, $\mathbf{Y}(\rho_y,\ z_y)$ being the source and the field point, respectively, belonging to the surface generators on which Eqs.(5) and (6) are defined and $\varphi=\varphi_y-\varphi_x$. The angle ϕ_x takes the value 0, because it is assumed that the surface generator of the axisymmetric body lies on the X_1-X_3 plane. Thus, the angle ϕ_y is always the same with angle ϕ and corresponds to the angle of revolution of the field point ***y***. More details about the axisymmetric BEM formulation for acoustic and elastic problems can be found in the works of Tsinopoulos, Agnantiaris, Polyzos (1999) and Tsinopoulos, Kattis, Polyzos, Beskos (1999).

3 BEM formulation

3.1 Non-axisymmetric problems

Numerical solution of equation (2) in conjunction with equation (4) is possible, when the boundaries S^e and s (Fig. 1) of the problem are discretized into two-dimensional isoparametric elements with piecewise interpolants for the associated field functions. These interpolants may be constant, linear or quadratic. In the present work, 9-noded and 8-noded quadratic isoparametric elements are used. In case of smooth boundaries, the elements are continuous. When the boundaries present discontinuities, such as corners or edges, or when there are sudden changes in the boundary conditions between neighbouring elements, then the field values are interpolated in nodes, which are shifted inside the element and as a consequence the elements become partially or fully discontinuous, depending on how many sides of the element contain nodes, which are shifted inwards [Rego Silva (1994)].

As it is mentioned in the introduction, the use of the Burton and Miller integral equation (4), introduces a computational difficulty known as the $C^{(1)}$-continuity difficulty, which appears due to mathematical arguments. Specifically, equation (4) contains a hyper-singular integral, the second one in the right-hand side, which exists in the Hadamard finite part sense [Rego Silva (1994)]. In order this integral to exist, the function p should be Holder continuously differentiable [Colton, Kress (1983)]. From a computational point of view, this fact means that in order to interpolate properly the acoustic pressure p over a smooth boundary, elements that guarantee the continuity of the first derivative of p should be chosen. One such choice is the Ovehauser elements [Tanaka, Sladek, Sladek (1994), Sladek, Sladek (1999)], but these elements need more than one degree of freedom per node, leading thus to a large system of equations to be solved. Another possible choice, but certainly more attractive than the previous one, is the choice of the fully discontinuous elements, mentioned above, where all the nodes used for the interpolation of the pressure field are inside the element where the continuity of the derivative is given. However, this choice is still uneconomical since every element on a smooth surface introduces no less than 8 degrees of freedom, for a typical 8-noded quadratic element, leading to large amount of equations, as compared with the use of continuous elements. Of course, there is always the alternative of choosing constant elements, which also guarantee the derivative continuity requirement, but at the cost of low-order spatial and field interpolation.

A good alternative to all the above mentioned techniques is the modified Burton and Miller algorithm (MBMA) first proposed by Ingber and Hickox (1992). According to this algorithm, also adopted in the present work, 9-noded quadratic continuous elements are employed and the SHIE (3) is written at the inter-element nodes, while equation (4) is written at the interior (9^{th}) node, in order to generate the final system of equations. In this way, the derivative continuity requirement for Eq.(4) is fulfilled and the fictitious eigenfrequency problem is circumvented efficiently. Of course, this algorithm is not restricted to the use of only 9-noded quadratic elements since any element configuration with interior nodes can be also used.

Thus, in the present work, the interface s between the acoustic and the elastic spaces is disretized into 9-noded elements, while any other kind of quadratic continuous elements, such as 8-noded or triangular 6-noded ones, are used for the discretization of the internal elastic boundary S^e. The BEM collocation procedure makes use of the Burton and Miller integral equation (4) for the 9^{th} node

of each element, while collocation to all the remaining nodes is performed by applying the SHIE (3).

Let us now consider a given boundary mesh, which involves N_e+N_α total number of nodes for the elastic space, including the nodes lying on the elastic boundary S^e and those lying on the interface s and N_α nodes for the acoustic space, lying on the acoustic side of the interface s.By collecting the discrete equations for all the nodes, one obtains two uncoupled systems of equations, one for each space. For the elastic structure, the system is written as

$$[\mathbf{A}_e]\{\mathbf{u}_e\}+[\mathbf{A}_{e\alpha}]\{\mathbf{u}_{e\alpha}\}-[\mathbf{B}_{e\alpha}]\{\mathbf{t}_{e\alpha}\}=[\mathbf{B}_e]\{\mathbf{t}_e\} \tag{8}$$

while, for the acoustic domain is written as

$$[\mathbf{C}_\alpha]\{p_\alpha\}+[\mathbf{C}_{e\alpha}]\{p_{e\alpha}\}-[\mathbf{D}_{e\alpha}]\left\{\frac{\partial p_{e\alpha}}{\partial \mathbf{n}^\alpha}\right\}=\left\{p^i+\varepsilon\frac{\partial p^i}{\partial \mathbf{n}^\alpha}\right\} \tag{9}$$

In the above systems, the subscripts $e$and $e\alpha$ denote integral influences and vector or scalar quantities referring to the elastic boundary and the interface boundary, respectively. The final coupled system of equations is derived with the aid of the boundary conditions (1) and is written as

$$\begin{bmatrix} \mathbf{A}_e & \mathbf{A}_{e\alpha} & -\mathbf{B}^*_{e\alpha} \\ \mathbf{0} & \mathbf{D}^*_{e\alpha} & \mathbf{C}_{e\alpha} \end{bmatrix} \begin{Bmatrix} \mathbf{u}_e \\ \mathbf{u}_{e\alpha} \\ p_{e\alpha} \end{Bmatrix} = \begin{Bmatrix} \mathbf{B}_e\cdot\mathbf{t}_e \\ 0 \end{Bmatrix} + \begin{Bmatrix} \mathbf{0} \\ p^i+\varepsilon\frac{\partial p^i}{\partial \mathbf{n}^\alpha} \end{Bmatrix} \tag{10}$$

where

$$[\mathbf{B}_{e\alpha}]\{\mathbf{t}_{e\alpha}\}=[\mathbf{B}_{e\alpha}\cdot\mathbf{n}^\alpha]\{p_{e\alpha}\}=[\mathbf{B}^*_{e\alpha}]\{p_{e\alpha}\} \tag{11}$$

and

$$[\mathbf{D}_{e\alpha}]\left\{\frac{\partial p_{e\alpha}}{\partial \mathbf{n}^\alpha}\right\}=[\mathbf{D}_{e\alpha}]\{-\rho_0\omega^2\mathbf{u}_{e\alpha}\cdot\mathbf{n}^e\}=[\mathbf{D}^*_{e\alpha}]\{\mathbf{u}_{e\alpha}\} \tag{12}$$

The matrix of the final system in Eq.(10) have dimensions $(3(N_e+N_\alpha)+N_\alpha)\times(3(N_e+N_\alpha)+N_\alpha)$ and as soon as the rearrangement of the known and unknown quantities is carried out, the system is solved numerically via the LU decomposition algorithm [IMSL (1994)]. It should be noticed here that this matrix is in general ill-conditioned, so in order to provide a reliable solution it should be properly scaled. The scaling chosen in the present work is the one used in the work of Goswami and Rudolphi (1993). According to that work the submatrices $\mathbf{B}^*_{e\alpha}$ and $\mathbf{D}^*_{e\alpha}$are multiplied by the factors μ/l and l/μ, respectively, where μ is the elastic shear modulus and l is the maximum distance between two nodes on the discretized boundary.

3.2 Axisymmetric problems

For the numerical solution of the axisymmetric integral equations, the meridional line of the shell (see Fig. 2), is discretized into 3-noded quadratic isoparametric boundary elements. Corners or points on the symmetry axis z where ρ = 0 are treated by partially discontinuous elements. As it is shown in the work of Tsinopoulos, Agnantiaris, Polyzos (1999), the proposed here axisymmetric boundary element methodology does not suffer from the $C^{(1)}$-continuity difficulty. Thus, Eq.(6) is collocated at all the nodes of the discretized boundary generator, in contrast with the aforementioned non-axisymmetric formulation, where the Burton and Miller equation is applied only for the middle node of a continuous 9-noded quadratic element. The integration over each element is performed numerically through standard Gauss integration on local basis. The integration over the circumferencial direction (Eq.(7)) is performed simultaneously for all the (n) harmonics of the problem, with the use of the FFT algorithm. Following the same steps as in paragraph 3.1, the final system of equations is the same with the one of Eq.(10), except that now, this system is valid for each of the expanding Fourier coefficients (n). As soon as the system is solved for each harmonic (n), the overall solution of the unknowns is obtained by Fourier synthesis over all the harmonics.

4 Evaluation of singular integrals

4.1 Weakly and strongly singular integrals

In the present work, the non-singular integrals over each element are evaluated numerically through the standard Gauss quadrature on local basis, utilizing a minimum of 5×5 integration points. When $\mathbf{x}\equiv\mathbf{y}$, the integral equations (2) and (4) become singular with various orders of singularity. More specifically, integral equation (2) contains a weakly singular integral $(O(1/r))$ and a strongly singular one $(O(1/r^2))$, with the later existing in the Cauchy principal value sense, corresponding to

the $\mathbf{u}^*(\mathbf{x},\mathbf{y})$ and $\mathbf{t}^*(\mathbf{x},\mathbf{y})$ kernels, respectively. Also, integral equation (4) contains weakly singular integrals and a hyper-singular integral ($O(1/r^3)$), which exists in the Hadamard' s finite part sense, corresponding to the second derivative of the Green' s function. In all cases, the singular integration is carried out directly, in terms of a local polar co-ordinate system, over the element on which the singular point belongs. This is accomplished with the aid of the highly accurate integration algorithms of Guiggiani (1992) and Guiggiani, Krishnasamy, Rudolphi, and Rizzo (1992) by making use of 6 Gauss points on both the local radial and polar directions.

In the axisymmetric BEM formulation, the singular integration, for every singular case is carried out in two steps. First, over a 3-D element created around the singular point, by also applying the aforementioned highly accurate integration algorithms and second over the rest of the circumferential direction, with the use of the non-periodic FFT algorithm. The singular integration method for Eqs.(5, 6) is described in detail in the works of Tsinopoulos, Kattis, Polyzos and Beskos (1999) and Tsinopoulos, Agnantiaris and Polyzos (1999).

4.2 Nearly-singular integrals

Considering a thin elastic shell, which is submerged into an infinite acoustic domain, a difficult situation to be dealt numerically is appeared. This difficulty concerns the numerical evaluation of the nearly singular integrals appearing in the SEIE, when a field point $\mathbf{x}$ is very close to the surface at which the integration is performed and the fundamental kernels of Eq.(2) grow rapidly in the rates of $O(1/r)$ and $O(1/r^2)$, respectively. The fact that makes this situation difficult to be treated is that the integration point does not belong to the same element with the field point $\mathbf{x}$, so limiting processes like those used by Guiggiani and co-workers for the singular case, are not straightforward applicable.

The simplest way to evaluate accurately nearly singular integrals is to determine the number of integration points, used in a standard Gauss quadrature, with the aid of simple relations giving the number Λ of a $\Lambda\times\Lambda$ total number of integration points over the element of integration. Such a relation has been established in the work of Tsinopoulos, Kattis, Polyzos and Beskos (1999) for the evaluation of strong nearly-singular integrals, with required integration accuracy of 0.01%. In the present work, a new similar formula is proposed for the numerical evaluation of the integrals with a desired accuracy of 0.001%. This formula is written as

$$\Lambda = \mathrm{INT}\left[1+2.53\cdot\left(\frac{D_{ek}}{l_e}\right)^{-1.08}\right], \tag{13}$$

where D_{ek} is the minimum distance between a field point $\mathbf{x}^k$ and an element e, l_e is the biggest element side and INT denotes the next lower integer. A study made in the framework of the present paper revealed that the above written relation proposes the use of 15×15 Gauss integration points for a D_{ek}/l_e ratio equal to 0.2, while for lower ratio values the number Λ grows rapidly leading to the use of 774×774 Gauss inegration points for D_{ek}/l_e=5×10^{-3}. As it is evident, the use of relation (13) for the accurate evaluation of nearly-singular integrals is acceptable, in terms of efficiency, only for ratio values greater than 0.2 and the minimum number of Gauss points proposed is 5×5. As a consequence this relation is adopted in the present work, only for $D_{ek}/l_e \geq 0.2$.

It is well known in the BEM community that for almost all categories of scattering problems, accuracy reasons impose a discretization rule, according to which, the maximum element side l_e, of all the quadratic elements of the mesh, should satisfy the relation $l_e \leq \lambda/4$, where λ is the wavelength of the acoustic excitation. Following this rule in the present work, the meshes resulted for the low to mid-frequency range, gave a minimum ratio D_{ek}/l_e of 5×10^{-3}. This means that the evaluation of the nearly singular integrals through the standard Gauss integration and the relation (13) becomes inefficient and thus the whole procedure should be replaced by another one which provides accuracy, as well as efficiency. The new procedure proposed here is more efficient from the previous one and it is described in detail in what follows. The integrals of Eq.(2) are written in the local co-ordinate system (ξ_1, ξ_2) of the element e as:

$$\mathbf{B} = \int_{-1}^{1}\int_{-1}^{1} \mathbf{u}^*\left(\mathbf{x}^k, \mathbf{y}^e(\xi_1,\xi_2)\right)\cdot N^{\alpha}(\xi_1,\xi_2)\cdot J(\xi_1,\xi_2)\, d\xi_1\, d\xi_2 \tag{14}$$

$$\mathbf{A} = \int_{-1}^{1}\int_{-1}^{1} \mathbf{t}^*\left(\mathbf{x}^k, \mathbf{y}^e(\xi_1,\xi_2)\right)\cdot N^{\alpha}(\xi_1,\xi_2)\cdot J(\xi_1,\xi_2)\, d\xi_1\, d\xi_2$$

(15)

where N^{α} are the quadratic shape functions, $\mathbf{y}^e$ is an integration point and $J(\xi_1,\xi_2)$ is the magnitude of the Jacobian of the transformation between the global and the local co-ordinate system. The integrals are further expressed in terms of the local polar co-ordinate system, with its origin located on the projection point $\mathbf{x}^p$, which is the point that belongs to the element e and is the nearest one to the field point $\mathbf{x}^k$. As it is evident, the amplitude $\left|\mathbf{x}^p-\mathbf{x}^k\right|$defines the minimum distance D_{ek} and the distance $\left|\mathbf{y}^e-\mathbf{x}^k\right|$, appearing in Eqs.(14) and (15), is equal to $D_{ek}+R$, with R being the radial co-ordinate of the local polar co-ordinate system. It should be noticed here that in the present formulation, the minimum distance D_{ek}, as well as the local co-ordinates $\left(\xi_1^p,\xi_2^p\right)$ of the projection point, are calculated accurately and efficiently, through the use of a quasi-Newton optimization algorithm, available in the IMSL numerical library [IMSL (1994)]. The integrals (14) and (15) are written now as:

$$\mathbf{B}=\sum_{m=1}^{l}\int_{\theta_1^m}^{\theta_2^m}\int_0^{R^{max}(\theta)}\mathbf{B}^m(R,\theta)\,R\,dR\,d\theta \tag{16}$$

$$\mathbf{A}=\sum_{m=1}^{l}\int_{\theta_1^m}^{\theta_2^m}\int_0^{R^{max}(\theta)}\mathbf{A}^m(R,\theta)\,R\,dR\,d\theta \tag{17}$$

where $\mathbf{A}^m$, $\mathbf{B}^m$ are the integrand quantities of integrals (15) and (14) expressed in the local polar co-ordinate system (R, θ). The integration is performed with the use of the standard Gauss quadrature and for this purpose the element is split into l triangles. The integration points are now defined on each triangle, over the radial R and the angular θ directions, respectively. As it is obvious from Eqs.(16, 17), the final value of the integral is the sum of the integrals over each triangle. In case when the projection point $\mathbf{x}^p$ belongs to more than one elements, then the final value of the integral is composed by summing the resulted integral values of all the related elements. This way of computing the nearly singular integrals has the advantage that the nearly singular behaviour of the kernels is taken into account along the radial polar co-ordinate only. As a consequence, the integration accuracy is depended only on the number of Gauss integration points over the radial (R) direction. Thus, the integration in Eqs.(16) and (17) is performed with the aid of a standard Gauss quadrature involving $K\times 4$ integration points, where K is the number of the radial integration points and is given by the relation

$$K=INT\left\{61.2+59.5\cdot\log\left[\left(1.-\left(\frac{D_{ek}}{l_e}\right)^{3.45\times10^{-5}}\right)^{0.617}+4.15\times10^{-3}\cdot\left(\frac{D_{ek}}{l_e}\right)^{-1}+0.124\right]\right\}. \tag{18}$$

This relation has been established through an optimization procedure, like that followed in the work of Tsinopoulos, Kattis, Polyzos and Beskos (1999), in order to evaluate nearly singular integrals with accuracy of 0.01 %. The maximum value of K is 116 for the minimum ratio value considered $D_{ek}/l_e=5\times10^{-4}$ and the minimum value of K is 8 for the maximum ratio value of 0.2. Considering the worst case of spliting an element e into 8 triangles (the projection point is located in the interior of the element e), the just described procedure with Eq.(18) proposes a total of $116\times4\times8$=3712 Gauss points for the evaluation of the nearly singular integral, which is a considerable improvement over the 774×774 Gauss points that Eq.(13) proposes, for even a greater ratio value (5×10^{-3}).

Similarly to the non-axisymmetric formulation, the numerical integration of nearly-singular integrals along the surface generator line, referring to Eq.(5), is performed with respect to the ratio D_{ek}/l_e, where now l_e is simply the length of the line element e. When the ratio is greater than 0.2, then the standard Gauss quadrature is performed, utilizing Λ integration points, with Λ given by the relation (13). The integration over the circumferencial direction is carried out through the FFT algorithm utilizing FFT points also given by optimized relations as they are provided in the works of Tsinopoulos, Kattis, Polyzos and Beskos (1999) and Tsinopoulos, Agnantiaris and Polyzos (1999). In order to follow the same procedure as in the non-axisymmetric formulation, when the ratio D_{ek}/l_e belongs in the interval [5×10^{-4}, 0.2] a 3-D boundary element *abcd* is created, with respect to the line element e of the discretized generator (see Fig. 3).

As described in Tsinopoulos, Agnantiaris and Polyzos (1999), the integrals of equation (5) are split into two integrals in the circumferential ϕ direction. One defined on the created 3-D element (-ϕ_e, ϕ_e) and the other over the remaining integration region (ϕ_e, 2π- ϕ_e). The angle ϕ_e is always an integer multiple of the angle step $\Delta\phi$, resulting by the division of the circumference into M seg-

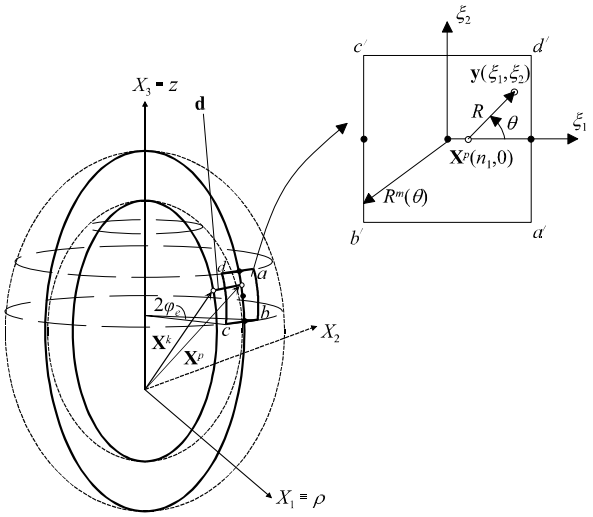

Figure 3 : 3-D Element around the nearly singular point

ments, and is calculated automatically, so one can write that $\phi_e = j\Delta\phi$. According to eq.(7) the integrals now become

$$\begin{aligned} \mathbf{U}^{(n)} &= \mathbf{U}^{(n)(1)} + \mathbf{U}^{(n)(2)} \\ \mathbf{T}^{(n)} &= \mathbf{T}^{(n)(1)} + \mathbf{T}^{(n)(2)} \end{aligned} \tag{19}$$

where

$$\left\{ \begin{array}{c} \mathbf{U}^{(n)(1)} \\ \mathbf{T}^{(n)(1)} \end{array} \right\} = \int_{-j\Delta\varphi}^{j\Delta\varphi} \left\{ \begin{array}{c} \mathbf{u}_c^* \left(\mathbf{X}^k, \mathbf{Y}(\xi_1), \varphi\right) \\ \mathbf{t}_c^* \left(\mathbf{X}^k, \mathbf{Y}(\xi_1), \varphi\right) \end{array} \right\} e^{in\varphi} d\varphi \tag{20}$$

$$\left\{ \begin{array}{c} \mathbf{U}^{(n)(2)} \\ \mathbf{T}^{(n)(2)} \end{array} \right\} = \int_{j\Delta\varphi}^{2\pi - j\Delta\varphi} \left\{ \begin{array}{c} \mathbf{u}_c^* \left(\mathbf{X}^k, \mathbf{Y}(\xi_1), \varphi\right) \\ \mathbf{t}_c^* \left(\mathbf{X}^k, \mathbf{Y}(\xi_1), \varphi\right) \end{array} \right\} e^{in\varphi} d\varphi$$

and $\mathbf{Y}(\xi_1)$ is an integration point on the line element, which is a function of its local co-ordinate ξ_1. The polar angle ϕ is expressed inside the 3-D element as a function of a second local co-ordinate ξ_2 as follows

$$\varphi(\xi_2) = j\Delta\varphi \cdot \xi_2, \quad \xi_2 \in [-1,\ 1]\,. \tag{21}$$

Thus, the integrals of eq.(5) are treated as surface integrals over the created 3-D element and their full expressions in the local co-ordinate system ξ_1-ξ_2 are the following

$$\mathbf{B}^{(n)(1)} = \int_{-1}^{1}\int_{-1}^{1} \rho_{\mathbf{Y}^e(\xi_1)} \left\{ \mathbf{u}^* \left(\mathbf{X}^k, \mathbf{y}^e(\xi_1,\xi_2)\right) \cdot \mathbf{D}\left(\varphi(\xi_2)\right) \right\} e^{in\varphi(\xi_2)} N^\alpha(\xi_1)\, J_\varphi J_{\xi_1} d\xi_1 d\xi_2 \tag{22}$$

$$\mathbf{A}^{(n)(1)} = \int_{-1}^{1}\int_{-1}^{1} \rho_{\mathbf{Y}^e(\xi_1)} \left\{ \mathbf{t}^* \left(\mathbf{X}^k, \mathbf{y}^e(\xi_1,\xi_2)\right) \cdot \mathbf{D}\left(\varphi(\xi_2)\right) \right\} e^{in\varphi(\xi_2)} N^\alpha(\xi_1)\, J_\varphi J_{\xi_1} d\xi_1 d\xi_2 \tag{23}$$

where $\mathbf{D}$ is the orthogonal transformation matrix relating the cylindrical and rectangular components of the fundamental solution tensors $\mathbf{u}^*$ and $\mathbf{t}^*$, N^α are the shape functions of the line element and $J_\phi = j\Delta\phi$ is the Jacobian of the transformation in eq.(19). In complete analogy to the non-axisymmetric formulation, those integrals are transformed into a local polar co-ordinate system, with origin located on the point $\mathbf{X}^p$ of the element e, which is the nearest one to the field point $\mathbf{X}^k$ (Fig.5). Following the latter transformation, the integrals are written as

$$\mathbf{B}^{(n)(1)} = \sum_{m=1}^{l} \int_{\theta_1^m}^{\theta_2^m} \int_0^{R^{max}(\theta)} \mathbf{B}^m(R,\theta)\, dR d\theta \tag{24}$$

$$\mathbf{A}^{(n)(1)} = \sum_{m=1}^{l} \int_{\theta_1^m}^{\theta_2^m} \int_0^{R^{max}(\theta)} \mathbf{A}^m(R,\theta)\, R dR d\theta, \tag{25}$$

where now $\mathbf{B}^m$ and $\mathbf{A}^m$ are the integrands of Eqs.(22) and (23), expressed in the local polar co-ordinate system. The numerical integration of Eqs.(24) and (25) follows exactly the same steps as the one for the non-axisymmetric case and is characterized by the same conclusions, meaning that Eq(18) is again used when $D_{ek}/l_e \in \left[5\times10^{-4}, 0.2\right]$. The circumferential integrals $\mathbf{U}^{(n)(2)}$ and $\mathbf{T}^{(n)(2)}$ are computed through a non-periodic FFT algorithm simultaneously for all the harmonics n.

5 Numerical examples

Two representative numerical examples concerning the acoustic wave scattering problems from axisymmetric elastic shells are solved here, in order to demonstrate the accuracy of the proposed BE methodology. The results of the present work are compared with analytically obtained solutions or numerical results taken by other investigators and useful conclusions about the solution convergence of such problems are provided.

5.1 Acoustic scattering by a spherical elastic shell

An elastic spherical shell made of steel (E=2.07×10^{11} Pa, ν=0.3 and ρ=7810. kg/m^3) is considered and is submerged into seawater (c=1500. m/sec, ρ_0=1026. kg/m^3). The shell is characterised by a thickness to radius ratio h/α = 0.01 and is exposed to a plane incident acoustic

wave travelling in the spherical co-ordinate direction (θ, φ) = (0 ˚ , 0 ˚), or alternatively, along the axis X_3 on the $-\hat{\mathbf{x}}_3$ direction. The back scattering amplitude, or else the form function, is computed for the range of dimensionless frequencies $k\alpha = 0 \div 8$. This problem exhibits symmetry on both the excitation and the geometry, with respect to the $X_1 - X_2$ and $X_1 - X_3$planes. Referring to the solution of the present scattering problem with the aid of the 3-D BEM formulation, one quarter of the internal and interface boundary surfaces is discretized into 90 8-noded and 9-noded (interface) quadratic continuous elements, respectively, as it is depicted in Fig. 4. This mesh provides a minimum D_{ek}/l_e ratio of 0.0573 and corresponds to 4 elements per wavelength with respect to the dimensionless frequency $k\alpha = 9$.

In order to solve the present problem with the aid of the axisymmetric BEM formulation, the half of the internal and the interface surface generator lines on the $X_1 - X_2$ of the spherical shell are discretized into 10 quadratic elements resulting to a minimum ratio $D_{ek}/l_e = 0.0636$. This mesh corressponds to 4 elements per wavelength with respect to the dimensionless frequency $k\alpha = 10$. The incident plane acoustic wave is now propagating along the spherical co-ordinate direction (θ, φ) = (90 ˚ , 0 ˚), or else, along the axis X_1 on the $-\hat{\mathbf{x}}_1$ direction. As it is evident the incident field in the present case is not axisymmetric over the circumferential φ direction, so more than one harmonic (n) are necessary for the solution on each frequency. The results obtained by using both formulations are compared with those obtained by the 3-D analytical solution, given in the work of Gaunaurd and Werby (1990), in figures. 5(a, b). The agreement between the present BEM and the analytical solution is excellent for the axisymmetric BEM and very good for the 3-D BEM, where a slightly denser mesh would correct the position of the two points lying on the first two resonance peaks.

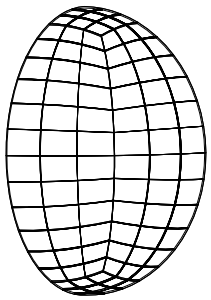

Figure 4 : One-quarter discretization of the shell boundary surface

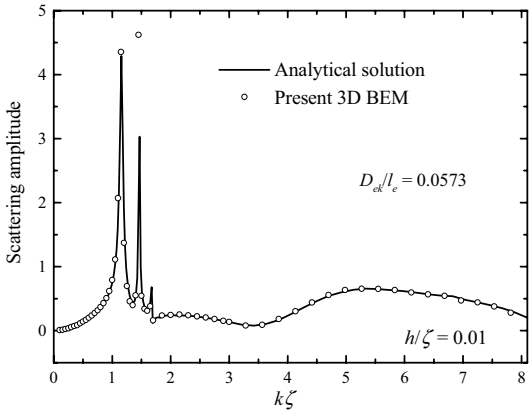

(a)

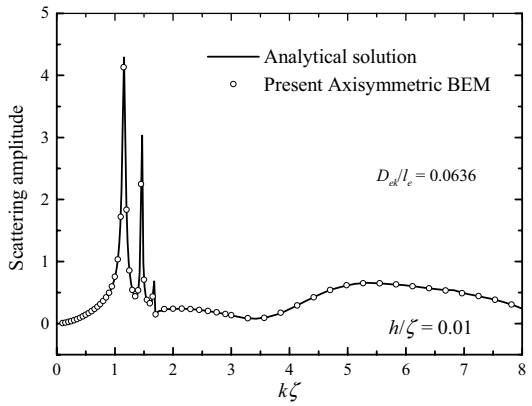

(b)

Figure 5 : Back scattering amplitude frequency response (a) 3-D BEM (b) Axisymmetric BEM

5.2 Acoustic scattering by a cylindrical shell with hemispherical endcaps

The present example concerns the acoustic plane wave scattering by a cylindrical shell with hemispherical endcaps. The two hemispherical endcaps of the shell are characterised by an internal radius b and an external one a and the relative thickness of the shell is $h=(a-b)/a$=0.03125. The relative length l of the shell's cylindrical part is taken as $l = L/\pi a$=0.5, where L is the length of the cylindrical part. In the present numerical example, the shell is made by aluminium (E=71.32 Gpa, v=0.33, ρ=2790 kg/m^3) and is immersed in water

(c=1470. m/sec, ρ_0=1000. kg/m^3). The incident plane acoustic wave impinges in a direction parallel to the axis of revolution zof the shell and as a result the incident field is axisymmetric, requiring thus only one harmonic for its accurate representation. This scattering problem has been recently attracted the interest of various researchers [Chen and Liu (1999); Maury, Filippi, Habault (1999); Veksler, Lavie and Dubus (2000)]. In the work of Veksler, Lavie and Dubus (2000), the problem is solved by employing the FEM for the motion of the elastic shell, while the infinite acoustic domain is modelled with aid of the BEM, based on the Helmholtz boundary integral equation. Both FEM and BEM are applied in an axisymmetric way and are solved in a coupled manner, with the BEM system of equations being over-determined by adding null-field equations, in order to avoid the fictitious eigenfrequencies difficulty.

This problem is solved here with the aid of the axisymmetric BEM formulation. The first mesh considered refers to a discretization of the internal and interface boundary surface generator lines into a total of 150 Elements. This mesh corresponds to 4 elements per wavelength with respect to a dimensionless frequency $k\alpha$ = 25, while the minimum D_{ek}/l_e ratio is 0.497. The resulting back scattering amplitude frequency response is plotted in Fig. 6 up to a dimensionless frequency $k\alpha$ = 5. In the same figure, the solution obtained by the FEM-BEM approach of Veksler, Lavie and Dubus (2000), under a 4 element per wavelength, with respect to a $k\alpha$ = 40 dimensionless frequency, discretization is co-plotted. As it is obvious, the current BEM solution does not represent with high accuracy the resonances existing at dimensionless frequencies $k\alpha \geq 3$.

Two additional discretizations are used which correspond to 4 elements per wavelength, with respect to the frequencies $k\alpha$ = 35 and $k\alpha$ = 40, or alternatively to ratios D_{ek}/l_e = 0.696 and D_{ek}/l_e = 0.796, respectively. The results are shown at Figs 7(a, b) and 8(a, b).

It is apparent from figures 7 and 8, that convergence have been already acccomplished with the use of the discretization, corresponding to the ratio D_{ek}/l_e=0.696. For the present example, the so far obtained results indicate that the accurate determination of the resonances occuring in the intermediate frequency range requires a boundary discretization which exceeds the usual 4 elements per wavelength criterion. Specifically, the present example showed that in order to represent with high accuracy the resonance peaks existing up to the dimensionless frequency $k\alpha$ = 5 the discretization must result to 28 elements per wavelength, with respect to this frequency. Furthermore, it can be seen that the ratio D_{ek}/l_e = 0.696, corresponding to this mesh, is outside the region that special numerical methodologies are used for the accurate and efficient evaluation of the nearly singular integrals. In other words, this means that for the present discretization all the integrals, where $\mathbf{x}\neq\mathbf{y}$, become regular. The immediate conclusion is that for the present example, specific efficient algorithms for the evaluation of the nearly singular integrals are only needed when the frequency range of interest is small ($k\alpha$¡ 3) or when the relative thickness of the scatterer is extremely small (h/α¡ 0.01).

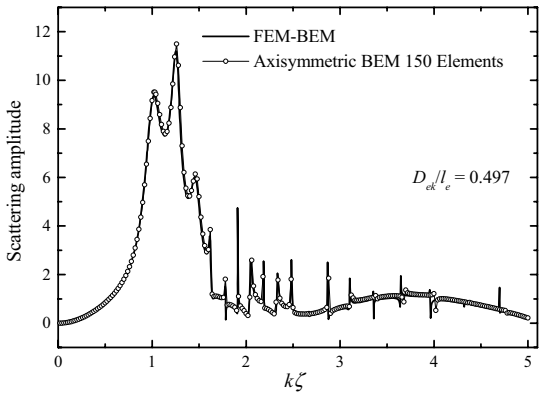

Figure 6 : Back scattering amplitude frequency response for cylindrical shell with hemispherical endcaps (150 Elements)

In order to compare the rate of convergence of the current BEM solution referring to the present non-spherical scatterer shape to the convergence rate of the solution of a corresponding spherical one, a second auxiliary problem is solved. This problem concerns the acoustic scattering by a spherical shell of the same thickness and material as those characterising the cylindrical shell with the hemispherical endcaps. The half of both surface generator lines is discretized similarly to the hemispherical endcaps generators part, meaning that 4 elements per wavelength are used, with respect to $k\alpha$ = 25. Also in the present case more than one harmonic are taken into account in the analysis. The latter mesh results to a total number of 50 elements and figures 9(a, b) depict the form function resulted by the present axisymmetric BEM for the frequency ranges $k\alpha$ =0÷5 and $k\alpha$ =0÷25, respectively.

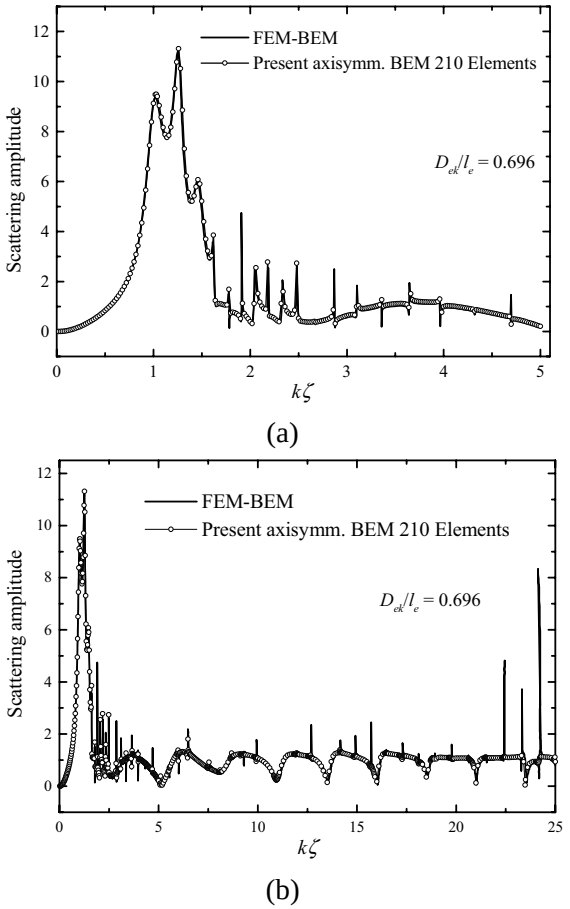

Figure 7 : Back scattering amplitude frequency response for cylindrical shell with hemispherical endcaps (210 Elements) (a) $k\alpha$ =0÷5, (b) $k\alpha$ =0÷25

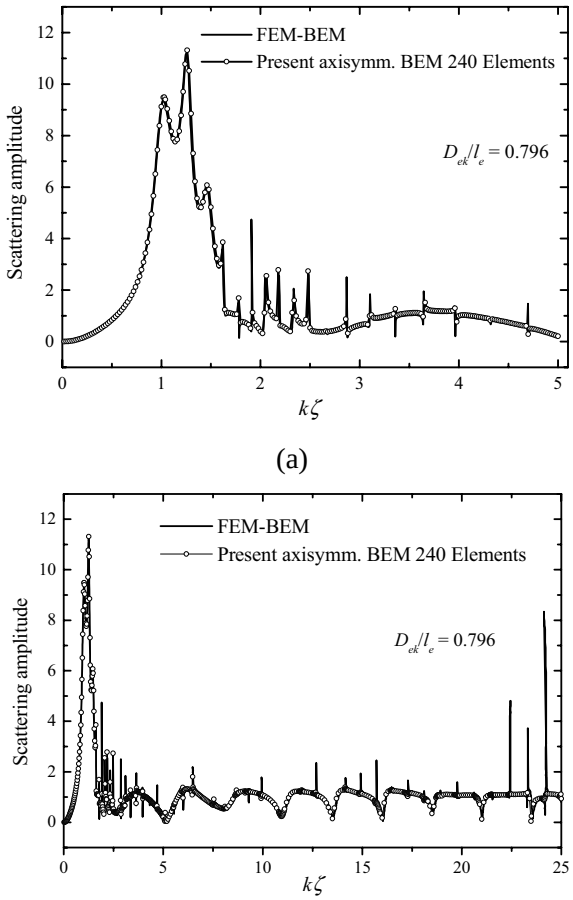

Figure 8 : Back scattering amplitude frequency response for cylindrical shell with hemispherical endcaps (240 Elements) (a) $k\alpha$ =0÷5, (b) $k\alpha$ =0÷25

The agreement between the present results to those obtained by the analytical solution [Gaunaurd and Werby (1990)] is excellent.

Furthermore, the same spherical shell problem is solved again by using a denser discretization, which results to 4 element per wavelength, with respect to $k\alpha$ = 40 (80 elements in total), and the results depicted in Figs. 10(a, b), for the same two frequency ranges as before, verify that convergence has been achieved.

Further investigation has shown that, for the present problem of the spherical shell, convergence can be accomplished with coarser discretization than that corresponding to $k\alpha$=25. The difference in the convergence of the two problems considered in the present paragraph can be explained as follows:

Comparing the figures 7 and 9 one can see that the back scattering amplitude of the spherical shell does not appear any significant resonance peaks at the intermediate frequencies as in the case of the cylindrical shell with the two hemispherical endcaps. Thus, the correct location of the intermediate resonances requires a denser discretization than that proposed by the standard 4 elements per wavelength criterion.

6 Conclusions

In the present work, a general-purpose acoustic-elastic interaction BEM formulation is presented. This formulation is capable of solving acoustic scattering problems by elastic shells, either being axisymmetric or non-axisymmetic, with high accuracy. Its main advantage, is that it makes use of the integral equations, for both the elastic and acoustic fields, in their direct form, avoiding

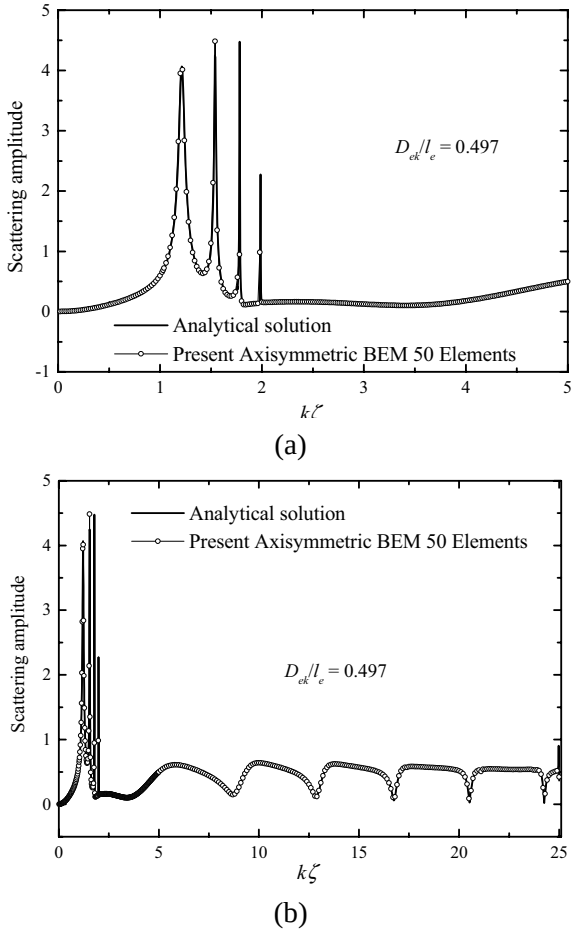

Figure 9 : Back scattering amplitude frequency response for the spherical shell (50 Elements). (a) $k\alpha$ =0÷5, (b) $k\alpha$ =0÷25

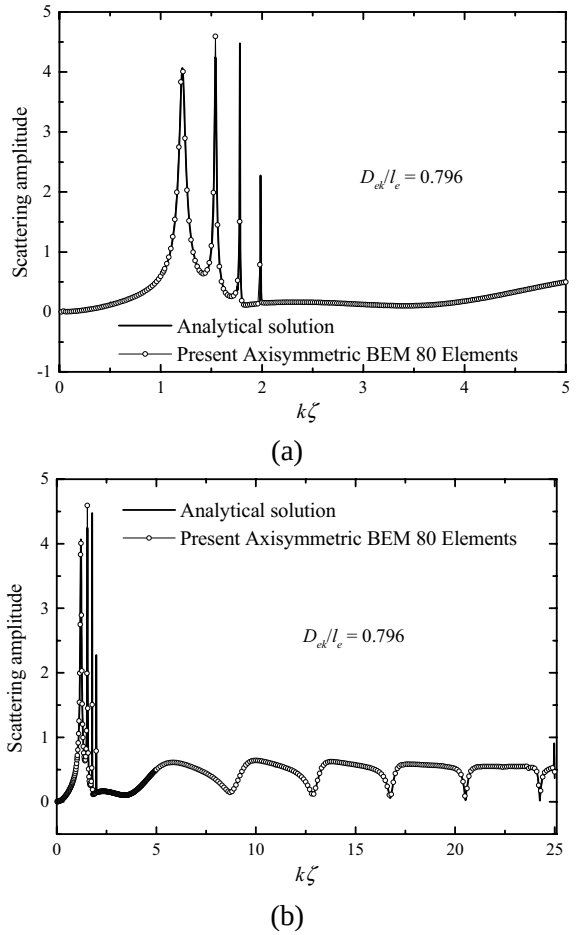

Figure 10 : Back scattering amplitude frequency response for the spherical shell (80 Elements). (a) $k\alpha$ =0÷5, (b) $k\alpha$ =0÷25

thus any *"a-priori"* regularization. ¿From a computational point of view, an effort has been made to numerically implement the system of the direct boundary integral equations in the most possible efficient way. In the context of this effort, useful observations and conclusions, concerning the crucial issue of treating the nearly singular integrals in the BEM, were presented. The numerical results clearly demonstrate the accuracy of the present formulation. Furthermore, it has been observed that for arbitrarily shaped shell scatterers of average thickness (0.01¡h/α¡ 0.05) the accurate prediction of the back scattering resonances at the intermediate frequencies through the BEM requires a denser discretization than that proposed by the well known 4 elements per wavelength criterion. The latter observation leads to the conclusion that efficient treatment of nearly singular integrals is useful when the frequencies of interest are low ($k\alpha$¡ 3), or when the elastic shell is very thin (h/α¡ 0.01).

Acknowledgement: The authors are grateful to the Greek General Secretariat of Research and technology for supporting this work under contract 95EΔ-5737 (YPER Programme).

References

Burnett, D. S.; Holford, R. L. (1998): Prolate and oblate spheroidal acoustic infinite elements. *Comput. Methods in Appl. Mech. And Engineering*, vol. 158, pp.117-141.

Burton, A. J.; Miller, G. F. (1971): The application of integral equation methods to the solution of some exterior boundary-value problems. *Proc. R. Soc. London Ser.*, Vol. A **323**, pp. 201-210.

Chen, S.; Liu, Y. (1999): A unified boundary element method for the analysis of sound and shell like structure interactions. I. Formulation and verification, *Journal of the Acoustical Society of America*, vol. 106(3), pp.1247-1254.

Chien, C. C.; Rajiyah, H.; Atluri, S. N. (1990): An effective method for solving integral equations in 3-D acoustics, *Journal of the Acoustical Society of America*, vol. 88, pp. 918-937.

Ciskowski, R. D.; Brebbia, C. A. (1991): *Boundary Element Methods in Acoustics*, Computational Mechanics Publications, Southampton, Boston and Elsevier Applied Science, London, New York.

Colton, D.; R. Kress (1983): *Integral Equation Methods in scattering theory*, Wiley-Interscience, New York.

Cooley, J. W.; Tukey, J. W. (1965): An algorithm for the machine calculation of complex Fourier series, *Math. Of Comput.*,vol. 19, pp. 297-301.

Cunefare, K. A.; Koopmann, G.; Brod, K. (1989): A boundary element method for acoustic radiation valid for all wavenumbers, *Journal of the Acoustical Society of America*, vol. 85, pp. 39-48.

Everstine, G. C.; Henderson, F. M. (1990): Coupled finite/boundary element approach for fluid-structure interaction, *Journal of the Acoustical Society of America*, vol. 87(5), pp. 1938-1947.

Gaul, L.; Fischer, M.; Nackenhorst, U. (2002): FE/BE Analysis of structural dynamics and sound radiation from rolling wheels, *CMES: Computer Modeling in Engineering & Sciences*, Vol. 3(6), pp. 815-823.

Gaunaurd, G. C.; Werby, M. F. (1990): Acoustic Resonance Scattering by submerged elastic shells, *Applied Mechanics Reviews*, vol. 43(8), pp. 171-208.

Goswami, P. P.; Rudolphi, T. J. (1993): Numerical simulation of ultrasonic transmission through curved interface, *Int. Journal for Num. Meth. In Engng*, vol. 36, pp. 2369-2393.

Guiggiani, M.; Krishnasamy, G.; Rudolphi, T. J.; Rizzo, F. J. (1992): A General Algorithm for the Numerical Solution of Hypersingular Boundary Integral Equations, *Journal of Applied Mechanics, ASME*, vol. 59, pp. 604- 614.

Guiggiani, M. (1992): Computing principal-value integrals in 3-D BEM for time-harmonic elastodynamics – a direct approach, *Commun. Appl. Num. Meth*, vol. 8, pp. 141-149.

Huang, Q.; Cruse, T. A. (1993): Some notes on singular integral techniques in boundary element analysis, *Int. Journal for Num. Meth. In Engng*, vol. 36, pp. 2643-2659.

Huber, C. J.; Rieger, W.; Haas, M.; Rucker, W. M. (1997): The treatment of singular integrals in boundary element calculations, *Applied Computational Electromagnetics Society Journal*, vol 12(2), pp. 121-126.

IMSL (1994): *IMSL Math/Library User's Manual, Version 3.0*, Visual Numerics, Inc., Houston, Texas.

Ingber, M. S.; Hickox, C. E. (1992): A modified Burton-Miller algorithm for treating the uniqueness of representation problem for exterior acoustic radiation and scattering problems, *Engineering Analysis with Boundary Elements*, vol. 9, pp. 323-329.

Krishnasamy, G.; Rizzo, F. J.; Liu, Y. J. (1994): Boundary integral equations for thin bodies, *Int. Journal for Num. Methods in Engng.*, vol. 37, pp. 107-121.

Lachat, J. G.; Watson, J. O. (1976): Effective numerical treatment of boundary integral equations: a formulation for three-dimensional elastostatics, *Int. Journal for Num. Meth. In Engng*, vol. 10, pp. 991-1005.

Lie, S. T.; Yu, G.; Zhao, Z. (2001): Coupling of BEM/FEM for time domain structural-acoustic interaction problems, *CMES: Computer Modeling in Engineering & Sciences*, Vol. 2(2), pp. 171-182.

Liu, Y. J. (1998): Analysis of shell-like structures by the boundary element method based on 3-D elasticity: Formulation and verification, *Int. Journal for Num. Meth. In Engng*, vol. 41, pp. 541-558.

Liu, Y. J. (2000): On the simple-solution method and non-singular nature of the BIE/BEM - a review and some new results, *Engineering Analysis with Boundary Elements*, vol. 24, pp. 789-795.

Liu, Y. J.; Rizzo, F. J. (1997): Scattering of elastic waves from thin shapes in three dimensions using the composite boundary integral equation formulation, *Journal of the Acoustical Society of America*, vol. 102, pp. 926-932.

Ma, H.; Kamiya, N. (2002): A general algorithm for the numerical evaluation of nearly singular boundary integrals of various orders for two- and three-dimensional elasticity, *Computational Mechanics*, Vol. 29, pp. 277-288.

Manolis, G. D.; Beskos, D. E. (1988): *Boundary Element Methods in Elastodynamics*, Unwin - Hyman, London.

Maury, C.; Filippi, P. J. T.; Habault D. (1999): Boundary integral equations method for the analysis of acoustic scattering from line-2 elastic targets, *Flow Turbulence and Combustion*, vol. 61, pp. 101-131.

Miller, R. D.; Thomas, E.; Moyer, J.; Huang, H.; Uberall, H. (1991): A comparison between the boundary element method and the wave superposition approach for the analysis of the scattered field from rigid bodies and elastic shells, *Journal of the Acoustical Society of America*, vol. 89, pp. 2185-2196.

Mukherjee, S.; Chati, M. K.; Shi, X. (2000): Evaluation of nearly singular integrals in boundary element contour and node methods for three-dimensional linear elasticity, *Int. Journal of Solids and Structures*, vol. 37, pp. 7633-7645.

Rego Silva, J. J. (1994): Acoustic and Elastic Wave Scattering using Boundary Elements, in *Topics in Engineering Vol. 18*, edited by C. A. Brebbia and J. J. Connor, Computational Mechanics Publications, Southampton, Boston, Chap. 2,3, pp. 7-68.

Schenk, H. A. (1968): Improved integral formulation for acoustic radiation problems, *Journal of the Acoustical Society of America*, vol. 44, pp. 41-58.

Schenk, H. A.; Benthien, G. W. (1989): The application of a Coupled Finite-Element Boundary-Element Technique to Large-Scale Structural Acoustic Problems, in *advances in Boundary Elements Vol. 2: Field and Fluid flow solutions*, edited by C. A. Brebbia and J. J. Connor, Computational Mechanics Publications, Southampton, Boston, pp. 310-317.

Seybert, A. F.; Rengarajan, T. K. (1987): The use of CHIEF to obtain unique solutions for acoustic radiation usingboundary integral equations", *Journal of the Acoustical Society of America*,vol. 81, pp. 1299-1306.

Seybert, A. F.; Wu, T. W.; Wu, X. F. (1988): Radiation and scattering of acoustic waves from elastic solids and shells using the boundary element method, *J. Acoust. Soc. Am.*,vol. 84, pp. 1906-1912.

Sladek, V.; Sladek, J. (1999): Modified Overhauser elements for approximation of boundary densities in regularized BEM formulations, *Computers and structures*, vol 73, pp. 161-176.

Sladek, V.; Sladek, J.; Tanaka, M. (2000): Optimal transformation of the integration variables in computation of singular integrals in BEM, *Int. Journal for Num. Meth. In Engng*, vol. 47, pp. 1263-1283.

Tanaka, M.; Sladek, V.; Sladek, J. (1994): Regularization techniques applied to boundary element methods, *Applied Mechanics Reviews*,vol. 47, pp. 457-499.

Telles J. C. F. (1987): A self-adaptive co-ordinate transformation for efficient numerical evaluation of general boundary element integrals, *Int. Journal for Num. Meth. In Engng*, vol. 24, pp. 959-973.

Tobocman, W. (1985): Comparison of the T-matrix and Helmholtz integral equation methods for wave scattering calculations, *Journal of the Acoustical Society of America*, vol. 77(2), pp. 369-374.

Tsinopoulos, S. V.; Kattis, S. E.; Polyzos, D.; Beskos, D. E. (1999): An advanced Boundary Element Method for axisymmetric elastodynamic analysis, *Computer methods in applied mechanics and engineering*. vol 175, pp. 53-70.

Tsinopoulos, S. V.; Agnantiaris, J. P.; Polyzos, D. (1999): An advanced Boundary Element/fast Fourier transform axisymmetric formulation for acoustic radiaton and wave scattering problems, *Journal of the Acoustical Society of America*, vol. 105(3), pp. 1517-1526.

Veksler, N. D.; Lavie, A.; Dubus, B. (2000): Peripheral waves generated in a cylindrical shell with hemispherical endcaps by a plane acoustic wave at axial incidence, *Wave motion*, vol. **31**, pp. 349-369.

Waterman, P. (1969): New foundations of acoustic scattering, *Journal of the Acoustical Society of America*,vol. 45, pp. 1417-1929.

Wilde, A. J.; Aliabadi M. H.; Power H. (1996): Application of a $C^{(0)}$ continuous element to the hypersingular integrals, *Boundary element Communications*, vol. 7, pp. 109-114.

Yang, S. A. (2000): An investigation into integral equation methods involving nearly singular kernels for acoustic scattering, *Journal of Sound and Vibration*, vol. 234(2), pp. 225-239.

Zeng, X.; Zhao, F. (1994): A coupled FE and Boundary Integral Equation method based on exterior domain decomposition for fluid-structure interface problems, *Int. Journal of Solids and Structures*, vol. 31(8), pp. 1047-1061.